Journal of Hydrology 566 (2018) 531–545

Contents lists available at ScienceDirect

Journal of Hydrology

journal homepage: www.elsevier.com/locate/jhydrol

Trends in hydrological extremes in the Senegal and Niger Rivers

Catherine Wilcox[a], Théo Vischel[a,*], Gérémy Panthou[a], Ansoumana Bodian[b], Juliette Blanchet[a], Luc Descroix[d], Guillaume Quantin[a], Claire Cassé[c], Bachir Tanimoun[e], Soungalo Kone[e]

[a] Univ. Grenoble Alpes, IRD, CNRS, Grenoble INP, IGE, 38000 Grenoble, France
[b] Laboratoire Leidi, Université Gaston Berger, Saint Louis, Senegal
[c] GET (UMR5563 CNRS, IRD, Université Toulouse III), OMP, Toulouse, France
[d] UMR PALOC IRD/MNHN, LMI PATEO, IRD Hann, BP 1386 Dakar, Senegal
[e] Authorité du Bassin du Niger (ABN), Niamey, Niger

ARTICLE INFO

This manuscript was handled by A. Bardossy, Editor-in-Chief, with the assistance of Felix Frances, Associate Editor

Keywords:
Floods
Flood hazard
West Africa
Non-stationarity
Extreme values
Model selection

ABSTRACT

In recent years, West Africa has witnessed an increasing number of damaging floods that raise the question of a possible intensification of the hydrological hazards in the region. In this study, the evolution of extreme floods is analyzed over the period 1950–2015 for seven tributaries in the Sudano-Guinean part of the Senegal River basin and four data sets in the Sahelian part of the Niger River basin. Non-stationary Generalized Extreme Value (NS-GEV) distributions including twelve models with time-dependent parameters plus a stationary GEV are applied to annual maxima of daily discharge (AMAX) series. An original methodology is proposed for comparing GEV models and selecting the best for use. The stationary GEV is rejected for all stations, demonstrating the significant non-stationarity of extreme discharge values in West Africa over the past six decades. The model of best fit most commonly selected is a double-linear model for the central tendency parameter (μ), with the dispersion parameter (σ) modeled as either stationary, linear, or a double-linear. Change points in double-linear models are relatively consistent for the Senegal basin, with stations switching from a decreasing streamflow trend to an increasing streamflow trend in the early 1980s. In the Niger basin the trend in μ is generally positive since the 1970s with an increase in slope after the change point, but the change point location is less consistent. The recent increasing trends in extreme discharges are reflected in an especially marked increase in return level magnitudes since the 1980s in the studied Sahelian rivers. The rate of the increase indicated by the study results raises urgent considerations for stakeholders and engineers who are in charge of river basin management and hydraulic works sizing.

1. Introduction

River floods are one of the deadliest natural hazards in the world. They produce major damages on infrastructure, lead to economic losses, and favor water-borne diseases. In order to better understand such floods, hydrologists have long focused on assessing the rare (large in magnitude) river discharge values, represented by the tails of underlying statistical distributions (Gumbel, 1957). The primary aim, besides theoretical understanding, is to provide practical tools for flood risk management and civil engineering structure design. The main challenge for practical applications is estimating return levels for high return periods (typically 10, 50, or 100 years). The more the return period is larger than the length of the series, the greater the challenge of estimating the tail of the distribution.

Extreme Value Distributions (EVDs) are statistical tools designed for the study of such rare values (see e.g. Coles et al., 2001; Katz et al., 2002). For several decades, the main challenge when applying EVDs was to have a proper estimation of the tail (heavy, light, or bounded). The focus was then on developing robust estimation procedures (Regional Frequency Analysis – Hosking and Wallis, 1997; GRADEX and adaptation – Guillot, 1993; Paquet et al., 2013; Bayesian inference – Coles and Tawn, 1996 among many other developments) and then applying them to the longest hydrological series available (Koutsoyiannis, 2004). The stationarity assumption reigned during this "old hydrological world" (Milly et al., 2008).

However, both increases and decreases of extreme discharges have been reported via the evaluation of historical series around the world (e.g. Kundzewicz et al., 2005; Bower, 2010; Condon et al., 2015). A main challenge of hydrological extremes thus concerns the validity of the stationarity assumption and the implications of its rejection. Ongoing global changes are expected to increase flood hazard mainly through the intensification of the hydrological cycle due to global warming (Hirabayashi et al., 2013; Arnell and Gosling, 2016) and the degradation of land surfaces due to anthropic pressure (Brath et al.,

* Corresponding author.

https://doi.org/10.1016/j.jhydrol.2018.07.063
Received 5 March 2018; Received in revised form 22 June 2018; Accepted 25 July 2018
Available online 05 September 2018

2006; Elmer et al., 2012). Other factors also tend to reduce flood hazards, including negative precipitation trends found in drying regions and flood protection structures such as dams. While some regions witness resulting changes in flood frequency, in other regions, no changes have been detected (Villarini et al., 2009). This could be a result of either the absence of substantial changes in drivers that could trigger/influence flood trends or competing phenomena that act in opposite ways. It could also be due to the use of non-robust methodology to detect concrete changes in the EVD of discharge. The last case necessitates improved methods able to detect trends in series characterized by low signal to noise ratio.

While numerous studies on flood hazard evolution have been undertaken for developed countries, less has been done in the developing world. This is the case in particular over the tropics (Kundzewicz et al., 2005) which contain two thirds of the developing countries, including the poorest. Populations living in the tropics are notoriously vulnerable to climate hazards, including droughts and floods that can occur within the same year at a given place. Global changes are expected to strongly impact flood risks in the tropics with studies already reporting significant increases in the frequency of rainfall extremes (Allan et al., 2010; O'Gorman, 2012; Asadieh and Krakauer, 2015), land use/cover changes (Lambin et al., 2003; Erb et al., 2016), rapid rates of urbanization (Di Baldassarre et al., 2010), and increasing vulnerability of populations due to very high demographic growth; the population of the least developed countries is expected to double from now to 2050 (Population-Reference-Bureau, 2016). The strong internal variability of tropical climates, the lack of long-term hydrological observations, and the large uncertainty of climate projections in the tropics challenge the scientific community to provide reliable and relevant information to stakeholders so they can define suitable flood risk management strategies.

West Africa is one of the most critical tropical regions for examining hydrological non-stationarities as it is a region in which the issues described above are exacerbated. West Africa is known for having strong precipitation variability, especially at the decadal level (Nicholson, 2013). It underwent a devastating and long-lasting drought that abruptly started in the late 1960s and persisted through the 1970s and 1980s (Lamb, 1983; Barbé et al., 1997; Nicholson, 2000; Camberlin et al., 2002; Barbé et al., 2002; L'hote et al., 2002; Dai et al., 2004; Panthou et al., 2014; Bodian et al., 2011; Bodian et al., 2016). At the regional scale, this led to a decline in the flow of large rivers that was proportionally greater than the decrease in rainfall (Lebel et al., 2003; Andersen and Golitzen, 2005; Mahé and Paturel, 2009).

At the subregional scale however, two diametrically opposed hydrological behaviors were observed (Descroix et al., 2018). In the Sudano-Guinean subregion of West Africa (south of 12°N), a decrease in river flow was observed for small to regional scale catchments (Mahé et al., 2005; Descroix et al., 2009) until the 1970s and 1980s (Diop et al., 2017). The decrease in flow was attributed to a gradual drying up of the groundwater and thus a gradual decrease in the base flow of the rivers (Mahé et al., 2000; Mahé and Paturel, 2009). In the Sahelian region (belt between roughly 12°N and 16°N), runoff coefficients and runoff volumes increased despite the drought. This phenomenon – the so-called "Sahelian paradox" – was understood to have been caused by a change in surface conditions (Albergel, 1987; Descroix et al., 2009; Aich et al., 2015; Cassé et al., 2016). Droughts played a role in increasing surface crust and decreasing vegetation (Gal et al., 2017), which consequently increased runoff coefficients and counterbalanced the effects of drought (Boulain et al., 2009). Anthropogenic changes (including land use change) appear to be a major factor in some basins (Seguis et al., 2004; Li et al., 2007; Leblanc et al., 2008; Gal et al., 2017). Other factors such as an increase in the density of the drainage network may have played a role in the increase of flow (e.g. Favreau et al., 2009; Gal et al., 2017).

Since the early 1990s, both total rainfall and streamflow amounts have increased compared to the drought decades of the 1970s and 1980s, though they remain lower than in previous pre-drought decades (Lebel and Ali, 2009; Mahé and Paturel, 2009; Panthou et al., 2014; Tarhule et al., 2015; Diop et al., 2017). In the Sahel, the increase was accompanied by higher interannual variability (Ali and Lebel, 2009; Panthou et al., 2014) and overall persistence of drought conditions under certain indices (L'hote et al., 2002; Ozer et al., 2009). Of note is the increase in the intensity of rainfall during recent years (Ly et al., 2013; Panthou et al., 2014; Sanogo et al., 2015; Taylor et al., 2017). During the same period, an increase in the number and magnitude of extensive floods has been reported (Tarhule, 2005; Tschakert et al., 2010; Samimi et al., 2012; Sighomnou et al., 2013; Cassé and Gosset, 2015), causing extensive fatalities, damages, and population displacement. From the mean hydrographs of the Niger River at Niamey plotted for six decades from 1951 to 2010, Descroix et al. (2012) and Sighomnou et al. (2013) illustrated a strong increase in the intensity of the summer flood peak of the Sahelian tributaries during the 2000s, while the flood peaks coming from the remote Guinean tributaries and arriving at Niamey later in the year at Niamey were as low as in the 1970s. They also noted successive discharge records produced by Sahelian floods in 2010 and 2012, exceeding the Guinean flood.

The strong current and projected demographic growth in West Africa (Population-Reference-Bureau, 2016) is likely to increase the exposure of populations to floods, both from intensive and unplanned human settlements in flood-prone areas (Di Baldassarre et al., 2010), and from human-induced changes in land cover which affect runoff. Changes in hydrological extremes consequentially are particularly pressing for decision makers in West Africa, as the statistical tools used for infrastructure design have not been updated since the 1970s (Amani and Paturel, 2017). An improved quantitative understanding of how extreme flows are changing over time in the region has generated an urgent demand to design and manage structures such as dams and dikes and, as a result, aid in risk mitigation, as well as the development of hydroelectric energy and irrigation systems.

However there is still very little literature on quantifying extreme flow changes in West Africa. For Sudano-Guinean regions, Nka et al. (2015) found an overall decreasing trend that closely followed rainfall indices (although decreasing at a higher rate); this was the case for the Falémé branch of the Senegal River at Fadougou. When only a more recent time period is considered (since 1970), no significant trends were found in the Sudano-Guinean catchments, including the Falémé. Bodian et al. (2013) explored trends in annual maximum daily discharge (AMAX) values on the Bafing tributary of the Senegal River (Bafing Makana and Daka Saidou stations). They found that high points in the series occurred during the pre-drought period (1967 and 1955), whereas the minima of the AMAX occurred in 1984. Diop et al. (2017) found that extreme highs in the Bafing Makana series decreased by 18% over the series and especially since 1971, while extreme lows stayed stable. Aich et al. (2016) analyzed time series of AMAX values at several stations along the Niger River. They found that changes in AMAX series followed the decadal variability of mean annual precipitation over Guinean and Benue-area catchments (a wet period during 1950s and 1960s, followed by a dry period during 1970s and 1980s, and values close to the long-term mean after), while the floods produced by Sahelian tributaries have recorded a monotonic increase since the beginning of the 1970s. Nka et al. (2015) found positive trends in the extreme values of three Sahelian catchments studied (Dargol River at Kakassi, the Gorouol River at Koriziena, and the Goudebo River at Falagontou). They also found significant (Mann–Kendall test) increases in extreme values in both AMAX series and peak-over-threshold (POT) series for the Dargol River at Kakassi. Breaks in AMAX were detected in 1987, and for POT in 1993. Mean extreme values were found to be greater (twice as high) during the later subperiods.

The aim of this paper is to detect and quantify trends in extreme hydrological values in West Africa. Discharge series are analyzed in tributaries of the Niger and the Senegal rivers, two catchments that reflect two differing hydrological and climatic processes of the Sahelian and the Sudano-Guinean West Africa. The temporal evolution of the

Table 1
Annual maxima (AMAX) data used in the study.

Subbasin	Station	Area (km^2)	Years	Gaps	Missing years
			Senegal River		
Bafing	Bafing Makana	21290	1961–2015	0.00%	None
Bafing	Daka Saidou	15700	1954–2015	4.84%	1956, 1958, 2009
Bakoye	Oualia	84700	1955–2015	1.64%	1982
Falémé	Gourbassi	17100	1954–2015	1.61%	2013
Falémé	Kidira	28900	1951–2015	23.10%	1960, 1963, 1965–68, 1970, 1972–73, 1978, 1980–82, 1986, 2010
Senegal	Kayes	157400	1951–2015	3.08%	2011, 2013
Senegal	Bakel	218000	1950–2015	1.52%	2009
			Niger River		
Niger	Sahelian Niger River	125000	1953–2012	0.00%	None
Dargol	Kakassi	6940	1957–2015	16.90%	1961, 1989, 1994, 1996–97, 1999, 2000, 2002, 2004–05
Sirba	Garbe Kourou	38750	1956–2015	10.00%	1959, 1960–61, 2000, 2004–05
Gorouol	Alcongui	44850	1957–2015	16.90%	1960, 1990, 1993, 1996–99, 2001, 2004–05

AMAX series is assessed by exploring different Generalized Extreme Value (GEV) models that range from a stationary GEV (S-GEV) to more complex non-stationary GEV (NS-GEV) models. The following study proposes an original methodology for identifying the most significant model to represent the evolution of extremes for a particular data series. Notably, the retained model is accompanied by significance levels and estimates of uncertainty. The retained model is used to compute time-varying frequencies of extreme flows. These changes are represented by the evolution of flow return levels over the last fifty to sixty years. Our results thus have implications for operational applications, as the design and operation of hydraulic structures depend on the magnitude of a flood event at a given return period.

2. Region of study and data

2.1. West African hydro-climatic features

The climate of West Africa is controlled by the West African Monsoon. The rainfall belt roughly follows the seasonal migration of the position of the Intertropical Convergence Zone (ITCZ). During the boreal winter (December-February), the rainfall belt is located over the Gulf of Guinea at around 4°N. It moves northward during the spring and reaches its northernmost position during boreal summer (June-September). At the regional scale, it implies that the hydro-eco-climatic features vary along a roughly north/south gradient. The mean annual rainfall amount decreases from south to north, ranging from over 1500 mm near the southern Guinean coast ($\approx$5°N) to less than 250 mm over the lower Saharan desert limit ($>$ 18°N).

The Sudano-Guinean and Sahelian regions are distinguished by their mean annual rainfall: the Sudano-Guinean region extends between the 1300 mm and 750 mm isohyetal lines and the Sahel between 750 mm and 250 mm. The regions have different seasonal rainfall cycles during the monsoon period (bimodal for the Sudano-Guinean region and unimodal signal for the Sahel), but are both characterized by a main rainfall peak in boreal summer and a dry season in boreal winter. The two regions are also differentiated by their respective vegetation: dense vegetation featuring tree savannah, woodland, and tropical forest for the Sudano-Guinean region (Bodian et al., 2016); dry savannah and sparse bush in the Sahel.

These contrasts influence the dominant hydrological processes characterizing the two regions. The Sahelian hydrology is distinguished by the prevalence of Hortonian overland flow (Horton, 1933). In the event of precipitation, water infiltrates until the infiltration capacity of the soil is reached. As a consequence, runoff production is driven by the hydro-dynamic properties of soils at the surface. The excess rainfall then runs off into the drainage network. Groundwater flow plays a minor role in the contribution to streamflow, if any. Due to this, river basins located in the Sahelian region are more sensitive to changes in fine-scale rainfall intensity (Vischel and Lebel, 2007). To the south, on the other hand, the Sudano-Guinean catchments have primarily Hewlettian hydrological processes (Cappus, 1960; Hewlett, 1961; Hewlett and Hibbert, 1967). Both surface and subsurface flow contribute to streamflow due to the elevated hydraulic conductivity of soils (Descroix et al., 2009). Under the same climatic evolution, river basins in the Sudano-Guinean zone may be less responsive to changes in rainfall intensity than in Sahelian river basins (Gascon et al., 2015).

2.2. Study catchments and datasets

Our analysis of changes in extreme flows is based on data available on two contrasted hydro-systems in West Africa: the upper reaches of the Senegal River located within the Sudano-Guinean region, and the middle reaches of the Niger River located within the Sahelian region. Table 1 overviews the data selection for the study, and Fig. 1 displays a map of their locations.

2.2.1. Sudanian tributaries of the Senegal River

The second largest river in West Africa is the Senegal River. The Senegal River drains a basin of approximately 300,000 km^2 (Rochette, 1974), found within the borders of four countries which are (from upstream to downstream): Guinea, Mali, Senegal, and Mauritania. It is formed by the confluence of three affluents that take their sources from the Fouta Djallon highlands in Guinea: the Bafing, the Bakoye, and the Falémé. Due to the delayed contribution of groundwater, the annual flood peak occurs a few weeks later than in Sahelian Niger (Fig. 2), whose seasonal hydrological signal follows that of precipitation more closely.

Seven stations whose major contributions come from within the Sudano-Guinean region are analyzed for the Senegal River (including the Bafing, Falémé, and Bakoye affluents), covering a total drainage area of 218,000 km^2. Globally from upstream to downstream, the stations are as follows: The Bafing at Daka Saidou (1954–2015, 15,700 km^2) and Bafing Makana (1961–2015, 21,290 km^2); the Falémé at Gourbassi (1954–2015, 17,100 km^2) and Kidira (1951–2015, 28,900 km^2); the Bakoye at Oualia (1955–2015, 84,700 km^2), and the Senegal at Kayes (1951–2015, 157,400 km^2) and Bakel (1950–2015, 218,000 km^2). The last two (Kayes and Bakel) are located downstream of the Manantali dam whose construction was completed in 1988. The Bakel station's catchment area includes those of all other stations studied, and represents the quantity of water that flows into the downstream valley.

2.2.2. Sahelian tributaries of the Niger River

With a drainage area of 2,170,500 km^2, the Niger is the largest river in West Africa, although only around 1,400,000 km^2 of its surface is estimated to effectively contribute runoff to the Niger River (Tarhule et al., 2015). It originates in the Fouta Djallon highlands in Guinea

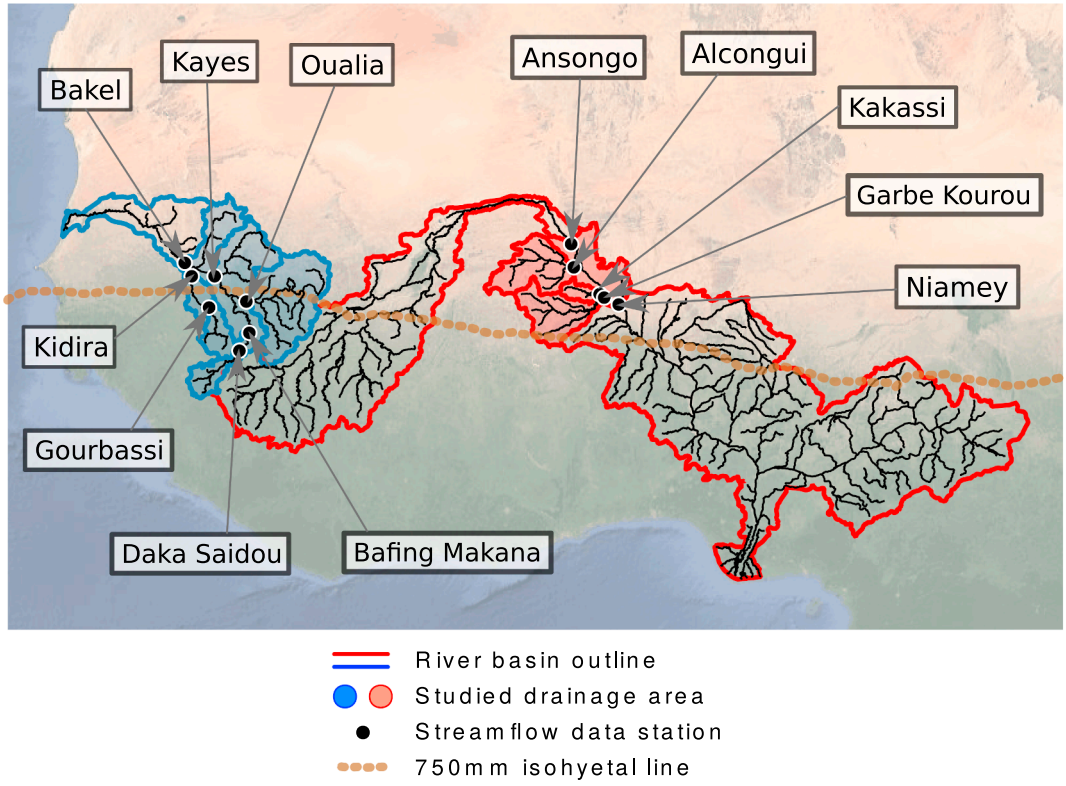

Fig. 1. Map of stations used in the study with their respective drainage basins (Boyer et al., 2006; Kahle and Wickham, 2013).

(Andersen and Golitzen, 2005). After spreading to form an inland delta in Mali, it reconverges and continues its course through the Sahelian region in Niger, crossing Benin and Nigeria before arriving at its outlet in the Gulf of Guinea. For the present study, analysis within the Niger basin focuses on the drainage area responsible for the Sahelian floods of the Niger River (Descroix et al., 2012; Cassé et al., 2016) that discharges its flows downstream of Ansongo and upstream of Niamey (Fig. 1), an effective drainage area of 125,000 km^2. An aggregated data set extracted from the difference between the Niger River streamflow series at Niamey and Ansongo during the local Sahelian rainy season (1953–2012 – see Cassé et al., 2016, for more details) represents this area for the subsequent analysis. This data series is hereafter referred to as the Sahelian Niger River (SNR) series. Fig. 2 shows the average seasonal signal of the SNR series.

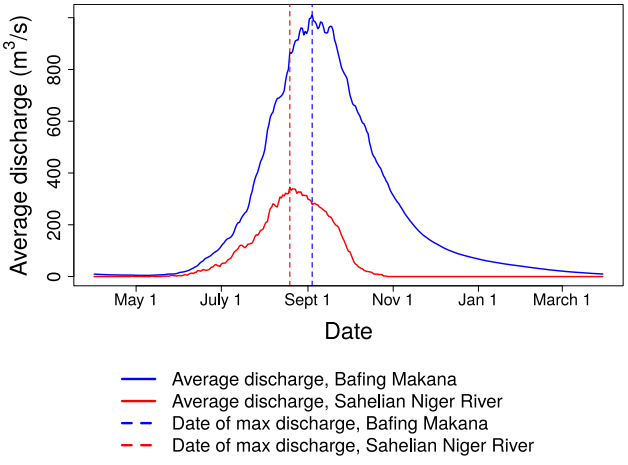

Fig. 2. Average seasonal signal for the Bafing Makana station in the Senegal River basin (blue) and the Sahelian Niger River (red). Period of record: 1961–2012. The flood peak has a smoother descent and occurs a few weeks later in the Senegal River basin due to the contribution of groundwater. (For interpretation of the references to color in this figure legend, the reader is referred to the web version of this article.)

The left bank of the Niger River within this catchment is largely endorheic. It only contributes to the Niger River during heavy rain events which generate small rivers that sporadically reach the main Niger River bed, although some evidence suggests that endorheic rupture is increasing in recent years (Mamadou et al., 2015).

The right bank of the Niamey-Ansongo reach consists of three major catchments: the Gorouol, the Sirba, and the Dargol, which together cover a total area of 90,540 km^2. Three data series are studied for these catchments: the Gorouol at Alcongui (1957–2015, 44,850 km^2), the Sirba at Garbe Kourou (1956–2015, 38,750 km^2), and the Dargol at Kakassi (1957–2015, 6,940 km^2). All three rivers are intermittent and only flow during the rainy season, following the general pattern seen in Fig. 2.

3. Theoretical framework and methodology

Extreme value distributions (EVDs) applied in a non-stationary context comprise some of the recent robust methods proposed for the detection of non-stationarity (Olsen et al., 1998; Cunderlik and Burn, 2003; Re and Barros, 2009; Marty and Blanchet, 2012; Park et al., 2011; Beguería et al., 2011; Panthou et al., 2013; Blanchet et al., 2016). Besides performing detection, EVDs also permit the quantification of trends and the evaluation of uncertainty. The principle of these methods is based on fitting EVDs both in stationary mode (stationary parameters) and in non-stationary mode (time-dependent parameters). The performance of the fitted models is then compared based on the capacity to accurately describe the data sample (goodness of fit) and the complexity of the model (parsimony). By searching for the most suitable temporal functions of parameter evolution, one can obtain an indication of the shape of the non-stationarity. The retained non-stationary model features vectors of parameters that best describe the data series in a statistically significant manner.

3.1. Selection of extreme discharge values

Extreme values can be defined as probabilistically rare occurrences, or values that are exceptionally large (or small) in magnitude. Extreme values can be extracted from a time series by two main approaches: by taking the maximum value within a given period, or by considering all values above a determined threshold. In this study – as in many climate and hydrological studies (see previous paragraph for examples) – extremes are defined as the maximum value of each year. A year is considered a long enough period for the extraction of maximum values for use in the subsequent analysis (Coles et al., 2001). At each station, the analyzed data series is formed by the annual maxima of daily discharge (AMAX).

The selected AMAX values were controlled for data quality. All eleven series span at least fifty years, which provides sufficient data points for the calibration of a statistical distribution. Data quality evaluation was focused on peak flow months. As demonstrated by West Africa's consistent seasonal signal (Fig. 2), the local rainfall-generated flood peak occurs on average within the months of August and September in both the Sahelian and Sudano-Guinean zones. Missing values before and after these months are unlikely to have an effect on the quality of the extreme flow data. On the other hand, a missing value during the peak streamflow months may have been the AMAX for that year. Identifying an incorrect data point as an extreme value would have an impact on the analysis.

With the potential impact of data quality in mind, the data series were evaluated. For the stations in the Senegal River basin, the year was removed from the series if any daily streamflow value was missing during the months of August and September. For stations in the Niger River basin, the hydrographs were viewed year by year. If values were missing near the flood peak, the year was removed. Years were also removed where recording errors that could affect flood peaks were perceived (for example, for one year it seemed that 100 m^3/s were added to all values).

Fig. 3 displays a sample of the AMAX data used, from the Bafing Makana station for the Senegal River (Fig. 3a) and SNR series for the Niger River (Fig. 3b). One can note that although there appears to be some trend, there is also a high degree of variability. The AMAX values at the Bafing Makana station started decreasing in magnitude in the 1960s and started increasing in approximately the 1980s. This visual trend was also found for the other Senegal stations. In Sahelian Niger, however, the increase appears to have begun earlier, during the drought years of the 1970s.

3.2. Formulation of statistical models

3.2.1. GEV distribution

A suitable statistical function used to represent the distribution of a random variable (Y) defined by block maxima is the GEV distribution (Coles et al., 2001), written as:

$$F_{GEV}(y;\mu,\sigma,\xi) = \exp\left\{-\left[1+\xi\left(\frac{y-\mu}{\sigma}\right)\right]^{-\frac{1}{\xi}}\right\} \text{ for } 1+\xi\left(\frac{y-\mu}{\sigma}\right) > 0 \quad (1)$$

where μ is the location parameter (a measure of central tendency), σ the scale parameter (a measure of dispersion), ξ the shape parameter (a measure of tail behavior), and y the value at which the GEV is to be evaluated.

The GEV distribution is fitted on AMAX series (y_i) with constant parameters (S-GEV, Eq. (2)) and various forms of time (t in years)-varying parameters (NS-GEV, Eq. (3)):

$$Y \sim \text{GEV}(\mu,\sigma,\xi) \quad (2)$$

$$Y \sim \text{GEV}\{\mu(t),\sigma(t),\xi(t)\} \quad (3)$$

3.2.2. Identifying appropriate temporal functions for GEV parameters

The implementation of one NS-GEV model requires choosing the general form of the appropriate temporal function for each GEV parameters. As there is no theoretical model for the time-dependent function, it must be assigned a priori. In order to determine a range of suitable functions, an initial exploration of trends is done by fitting S-GEV distributions in moving windows over the study periods. A window size of 15-years has been selected as a compromise between having sufficient data to fit the GEV and highlighting potential parameter evolution. Due to the difficulty in estimation, the parameter ξ was first calibrated using the entire data sample, then kept stationary while μ and σ change with each window.

Fig. 4 displays an example of the moving window for μ (4a) and σ (4b) for the Bafing Makana station. For this station, both parameters are characterized by a v-shaped pattern which is more distinct for μ than σ. Based on the moving window analysis for the 11 different stations, it was identified that μ and σ can be qualitatively described by one single or several connected linear segments. For all stations it was visually observed that changes in μ were more clearly defined than changes in σ. One can note here that the moving window method allows for qualitatively assessing the overall trends in GEV parameters. However, unlike NS-GEVs, the moving window does not allow for the quantification of the trend, nor its significance.

3.2.3. Formulation of GEV parameter temporal functions

According to the qualitative analysis derived from the moving window GEV, several temporal patterns with varying complexity were identified to describe the GEV parameters. Linear, double-linear (with one breakpoint), and triple-linear (with two breakpoints) temporal functions were considered for μ, σ, or both. In the case of both parameters varying, μ and σ were permitted to vary independently. As with the moving window, ξ was kept constant. A non-linear (polynomial) model was also considered initially, but showed no improvement over the multilinear models.

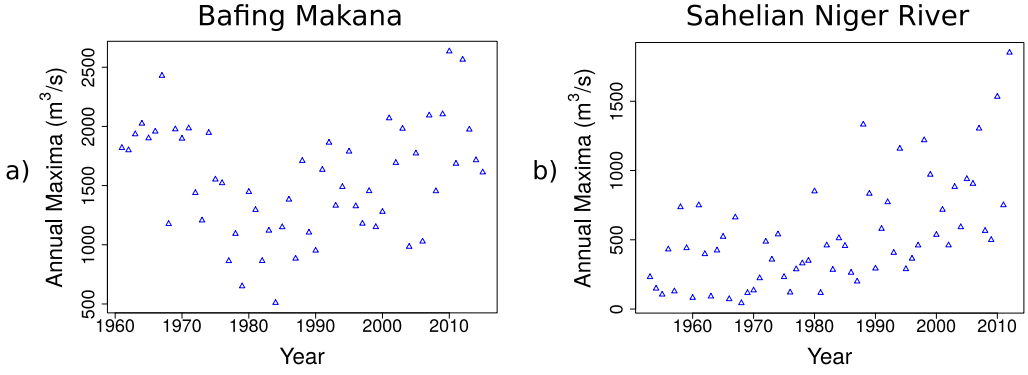

Fig. 3. Sample AMAX data from the Bafing Makana station in the Senegal River basin (a) and the Sahelian Niger River series (b).

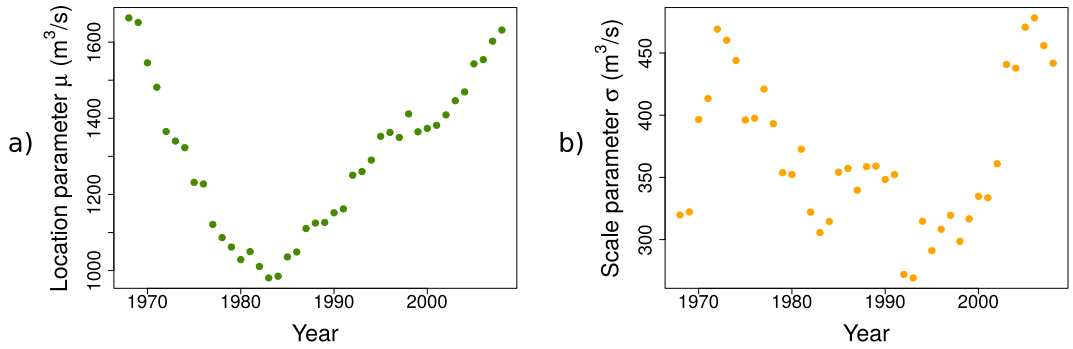

Fig. 4. Moving window estimates for the GEV distribution parameters μ (a) and σ (b) for the Bafing Makana station. The points represent the center of the fifteen-year window over which the parameters were estimated.

To represent this non-stationarity mathematically, we introduce the function $\eta(t)$, where η represents either μ or σ and t is a time-dependent covariate. $\eta(t)$ takes on different forms depending on the trend model:

Stationary parameter model:

$$\eta(t) = \eta_0 \tag{4}$$

This parameter model has only one degree of freedom, η_0.

Single-linear trend:

$$\eta(t) = \eta_0 + \eta_1 \times t \tag{5}$$

In this case $\eta(t)$ has two degrees of freedom: η_0 and η_1, and thus one additional degrees of freedom in comparison with a stationary parameter.

Double-linear trend:

$$\eta(t) = \eta_0 + \eta_1 \times (t - t_1) \text{ for } t \leqslant t_1 \tag{6}$$

$$\eta(t) = \eta_0 + \eta_2 \times (t - t_1) \text{ for } t_1 < t \tag{7}$$

t_1 represents the breakpoint in time (year index) where the two linear segments join (i.e. where the slope of the linear model changes). In this case $\eta(t)$ has four degrees of freedom: η_0, η_1, η_2 and t_1, meaning three additional degrees of freedom in comparison with a stationary parameter model.

Triple-linear trend:

$$\eta(t) = \eta_0 + \eta_1 \times (t - t_1) \text{ for } t \leqslant t_1 \tag{8}$$

$$\eta(t) = \eta_0 + \eta_2 \times (t - t_1) \text{ for } t_1 < t \leqslant t_2 \tag{9}$$

$$\eta(t) = \eta_0 + \eta_2 \times (t_2 - t_1) + \eta_3 \times (t - t_2) \text{ for } t_2 < t \tag{10}$$

In this case, $\eta(t)$ has six degrees of freedom: η_0, η_1, η_2, η_3, t_1, t_2.

A total of 13 different GEV models are considered: one with all parameters stationary (S-GEV) and 12 NS-GEV models that combine the above parameter trend models in Eqs. (4), (5), (7), (10) for μ and σ. They are reported in Fig. 5, classified according to their degrees of freedom.

3.3. Model fitting

For S-GEV, the parameters are directly fitted using maximum likelihood estimation (MLE). In the NS-GEV scenario, for each temporal function (linear, multi-linear), the following procedure is performed:

1. If the formulation includes one or two breakpoints, the year of each breakpoint t_i is defined before estimating the other parameters η_i:
   - In order to limit border effects, the breakpoint(s) must be positioned not earlier than 10 years after the beginning of the series and no later than ten year before the end. Likewise, two successive breakpoints must be separated by at least 10 years.
   - The breakpoints are defined independently for $\mu(t)$ and $\sigma(t)$, and can be at a different point in time (though not necessarily).

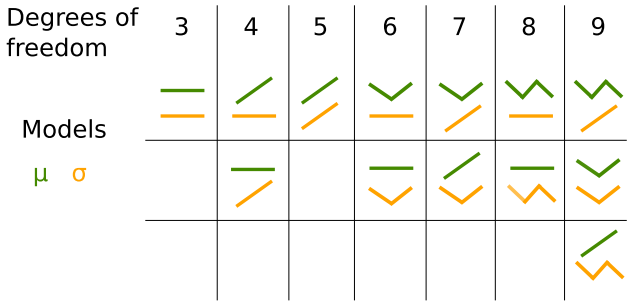

Fig. 5. Covariate models tested for GEV distributions.

2. At each defined breakpoint, the parameters η_i are estimated according to the formulations of $\eta(t)$ in Eqs. (4), (5), (7), (10) using MLE.
3. Repeat steps 1 and 2 until all possible breakpoint dates have been tested.
4. Retain the model that gives the maximum likelihood among the different breakpoint dates tested in steps 1 to 3.

3.4. Selection of the best GEV model

A more complex model may provide better fit, but not to a degree that merits additional parameterization. The selection of the best model is done by comparing the maximum likelihood obtained by the 13 different GEV models per station and evaluating their significance. The selection process consists of two steps: First, an initial best model is selected via the Akaike Information Criterion (AIC – Akaike, 1974). Then, the model choice is validated via a Likelihood Ratio Test (LRT – Coles et al., 2001). According to Kim et al. (2017), AIC and LRT are both suitable for evaluating non-stationary representations of hydrological data. AIC in particular is robust with small data sets.

The AIC balances model fit against model complexity in the following equation:

$$\text{AIC} = 2k - 2\log(L) \tag{11}$$

where k is the number of parameters in the model and L is the maximum likelihood value associated with the model. The model with the lowest AIC value is selected.

The LRT is a test between two models that must be "nested"; the simpler model is contained within the more complex models. While AIC compares all models globally, LRT validates the addition or subtraction of specific parameters. The likelihood ratio test (LRT) is performed by comparing the following statistic to the χ^2 distribution:

$$D = 2 \times \{\log[L(M_1)] - \log[L(M_0)]\} \tag{12}$$

where $\log[L]$ is the maximum value of the log likelihood of model M and M_0 is nested in M_1. If D exceeds the α-quantile of the χ^2 distribution with n degrees of freedom, with n the difference in the number of

parameters between the two models (additional degrees of freedom), then the more complex model is accepted at level α.

For this study, AIC is first used to find an initial model of best fit for each station. The model selection via AIC is then validated using LRTs. All models that are nested within the model selected via AIC are tested in pairs with the selected model using the LRT with $\alpha = 0.10$. This confirms that the added complexity is significant. More complex models that have the AIC selection as a nested model are likewise tested in pairs against the AIC selection using the LRT to validate the exclusion of additional parameters.

Note that the inclusion of the stationary GEV model in the comparison allows for the evaluation of the presence of a non-zero trend, accompanied by a significance level. If the selected model is an NS-GEV, then the stationary hypothesis is rejected.

3.5. Return level evaluation

The use of a parametric distribution for representing the data allows for the estimation of return levels r_T corresponding to return period T. The return level r_T is exceeded with a probability p in a given year where $p = 1/T$. The return levels can be calculated as follows:

$$r_T = \mu - \frac{\sigma}{\xi}\{1-[-\log(1-p)]^{-\xi}\} \tag{13}$$

For non-stationary models, the corresponding value of μ and σ for the NS-GEV are inserted in Eq. (13) at each time step in order to obtain the non-stationary return levels for a given p.

A comparison of the relative evolution of return levels was conducted using normalized return level values for each station. The normalization was conducted by dividing the values of the non-stationary return levels by the value r_T calculated under the stationary assumption (S-GEV).

$$r_{T,normalized} = \frac{r_T(NS-GEV)}{r_T(S-GEV)} \tag{14}$$

3.6. Uncertainty assessment

Confidence intervals for model parameters were determined via nonparametric bootstrapping (Efron, 1979; Efron and Tibshirani, 1994; Davison and Hinkley, 1997). While approximate confidence intervals can be calculated via approximation to the normal distribution, the approximation becomes less valid for the parameter ξ and for values at the tail of the distribution (high return periods). Thus, bootstrapping was selected as providing a more accurate representation of the uncertainty.

For each station, a data sample of equal length to the original series was extracted via resampling. An NS-GEV of the same model type and with the same breakpoint as the selected NS-GEV for the station was calibrated on the sample. This was repeated 500 times for each station. Samples were discarded if their NS-GEVs had a ξ value greater than 1 or less than -1, or if there were errors while estimating the NS-GEV and associated uncertainties, likely due to particularly skewed samples (same values selected many times, extreme values overselected, etc). Confidence intervals for the percentiles of interest were then calculated at each time step of the data series.

In the methodology used for this study, the breakpoints were fixed before performing MLE to estimate the NS-GEV parameters. The uncertainty evaluation methods detailed above assume that the uncertainty in breakpoint estimation is negligible compared to the uncertainty in the estimation of the other NS-GEV parameters (uncertainty of the η_i). This assumption is explored further in subsection 5.3.3.

4. Results

4.1. Selected GEV model

Table 2 shows the model of best fit that was selected for each station with a p-value (α) of 0.10 used in the LRT. One can note that for all stations, an NS-GEV model always fit the series of AMAX better than the stationary GEV model.

Fig. 6 visualizes an example of these models, with moving window parameter values (circles) and selected NS-GEV model μ values (line). Confidence intervals for μ are shown with dashed lines. One can see that the selected models follow the general trends seen in the moving window parameter estimation of μ.

A double linear model was selected for μ for all stations, with the exception of the Alcongui station in the Gorouol basin which was best represented by a linear model for μ (although a double linear model would have been accepted at $\alpha = 0.15$). The selection of a double linear model indicates that the slope of the trend for μ differed significantly between two subperiods of the time series.

In the Senegal River basin, significant breakpoints were consistently found for μ between 1980 and 1984 for all stations. The slope of the central tendency was negative (decreasing trend) during the period up until the early-mid 1980s, then became positive through the modern period. The changes in μ were less rapid in all stations during the latter period. Kayes and Bakel (the two stations downstream of the Manantali Dam) showed the least relative increase of all stations. Of the stations in the Senegal River basin, the Daka Saidou, Kidira, and Oualia stations demonstrated significant non-stationarity in the scale parameter (σ). All non-stationarity σ models were double linear. Daka Saidou's breakpoint for σ was in 2000, while Kidira and Oualia both occurred in the 1990s (1995 and 1994 respectively). This reflects the general decrease throughout the majority of the time period under study then rapid increase in variability seen in the moving window for σ during the 1990s at these stations.

For the Sahelian stations in the Niger River, all stations showed an increasing trend starting as early as the 1970s. However, the specific model characteristics were less homogeneous between the different stations than for the Senegal River stations. Although all models were double linear for μ, breakpoints for μ were found in the 1990 for the Dargol (at Kakassi) and 1997 for the Sirba (at Garbe Kourou). The slope of the trend was positive for both subperiods for these two stations, with a greater (more rapidly increasing) slope during the more recent period. For the SNR data series, the slope was gradually decreasing during the earlier period of record up until 1968, then increasing at a higher absolute magnitude during the more recent period. The Gorouol series (at Alcongui) was linearly increasing throughout the period for μ. The SNR and Sirba, series showed significant trends in the σ parameter. For the SNR series, the change in σ was determined to be linearly increasing. For the Sirba, the model for σ was double linear with a breakpoint in 1977. The models closely follow the moving window estimates.

4.2. Extreme discharge tails behavior

Table 2 also shows the most likely ξ values for each distribution. A heavy-tailed GEV distribution ($\xi > 0$) indicates that larger values are possible (and more probable than if $\xi = 0$). $\xi < 0$ means that the distribution is bounded; rare values will approach but not exceed a maximum threshold.

For the Senegal River, all ξ values were either close to zero (Gumbel distribution, unbounded but not heavy-tailed) or negative (Weibull distribution). Almost all ξ values for the Sahelian Niger basin stations were positive (Frechet distribution), which means the distribution of the values is heavy-tailed without an upper bound. The exception was the Gorouol station at Alcongui, which had a slightly negative ξ value (Weibull distribution, bounded). However, the 95% confidence

Table 2
Model selection, GEV analysis results, and associated confidence intervals (CI).

Subbasin	Station	GEV model	Breakpoints	ξ	ξ, 95% CI
Senegal River					
Bafing	Bafing Makana		1983 μ	-0.33	(-0.88, -0.12)
Bafing	Daka Saidou		1980 μ 2000 σ	-0.15	(-0.72, 0.51)
Bakoye	Oualia		1983 μ 1994 σ	-0.15	(-0.37, 0.48)
Falémé	Gourbassi		1983 μ	-0.06	(-0.41, 0.14)
Falémé	Kidira		1984 μ 1995 σ	-0.03	(-0.69, 0.49)
Senegal	Kayes		1984 μ	-0.03	(-0.40, 0.18)
Senegal	Bakel		1984 μ	-0.13	(-0.71, 0.05)
Niger River					
Niger	Sahelian Niger River		1968 μ	0.37	(-0.17, 0.87)
Dargol	Kakassi		1990 μ	0.14	(-0.17, 0.48)
Gorouol	Alcongui			-0.08	(-0.50, 0.28)
Sirba	Garbe Kourou		1997 μ 1977 σ	0.18	(-0.20, 0.70)

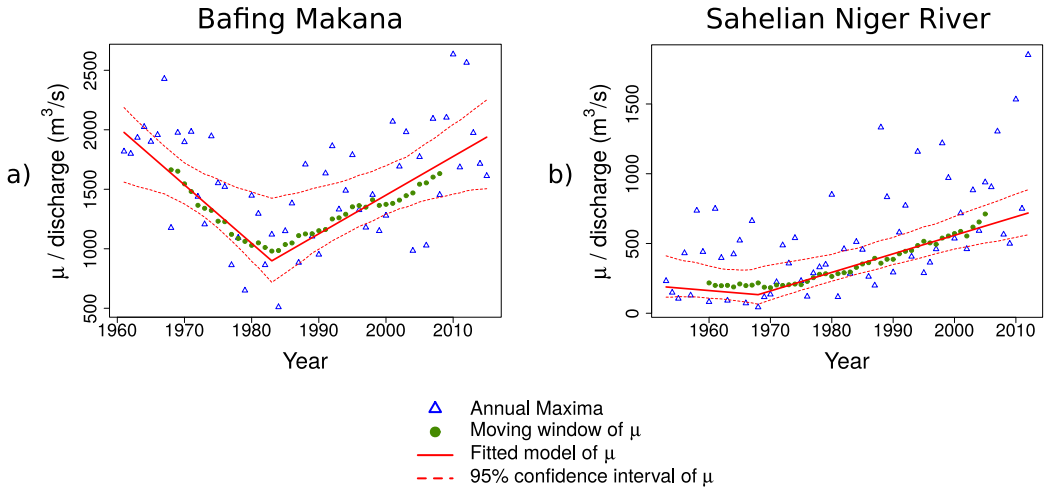

Fig. 6. NS-GEV model for the Bafing Makana station (a) and SNR data series (b) with raw AMAX values (triangles), moving window estimates (circles), μ evolution for the NS-GEV model (solid line), and 95% confidence intervals for μ for the NS-GEV model (dashed lines).

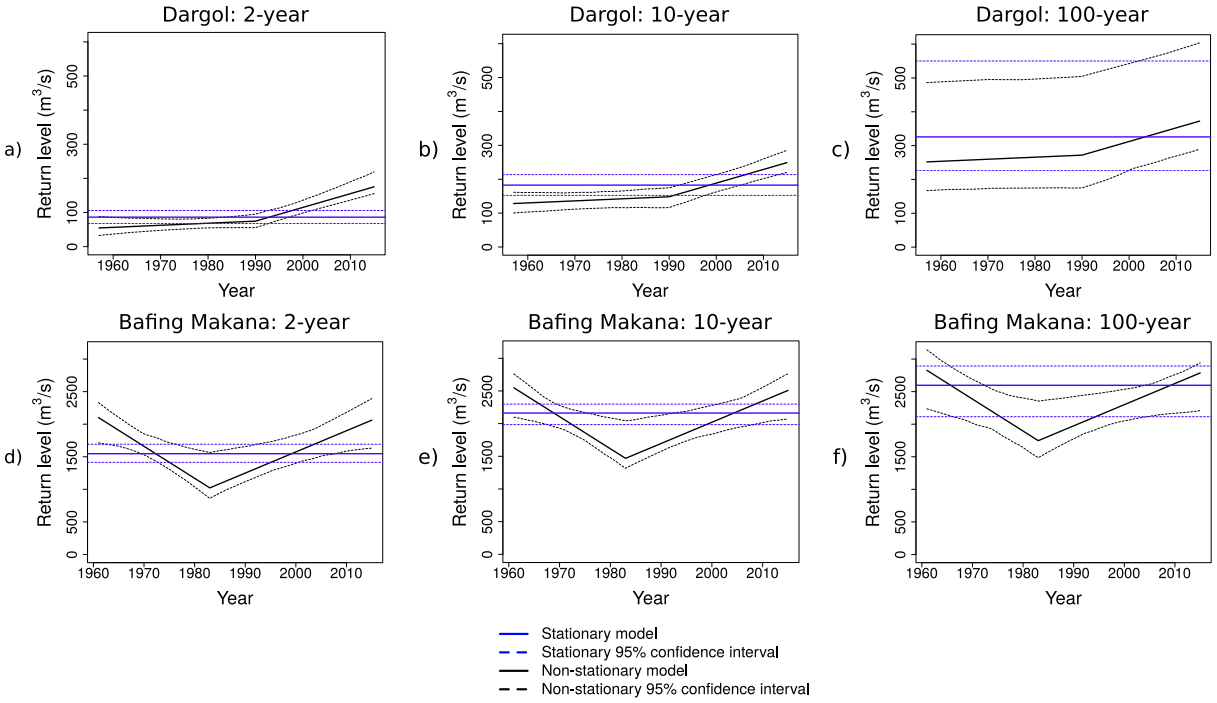

Fig. 7. 2-year, 10-year, and 100-year return level values for the Dargol (a–c) and Bafing Makana (d–f) stations, with the NS-GEV values compared to the stationary model. Note that the 95% confidence interval for the NS-GEV return level completely exceeds the confidence interval for the stationary model for the 2-year return level, but for the 100-year return level the confidence intervals of the stationary model and the NS-GEV largely overlap.

intervals for ξ for all stations in both river basins included both positive values and negative values, with the exception of the Bafing Makana station where the interval was entirely in the negative range (Weibull distribution).

4.3. Return level estimates of selected models

The main practical advantage provided by the NS-GEV models is the ability to estimate return levels from the fitted distribution. This is illustrated in Fig. 7 where 2, 10, and 100-year return levels are plotted with their 90% confidence intervals for the Bafing Makana and Dargol stations. Return levels in the Senegal basin followed the general pattern of Bafing Makana, first decreasing below the stationary level then increasing again. Return levels for the stations studied in the Niger River started increasing earlier than for the Senegal River.

Note the increase in the size of the confidence level with the longer return periods. For shorter (2 and 5-year) return periods, the confidence intervals for the non-stationary model were more likely to be distinctly higher than those of the stationary model. Especially at 10-year and longer return levels, the confidence intervals of the stationary and non-stationary models increasingly overlap. Fig. 8 demonstrates this separation and overlap between the confidence intervals of the stationary model and the chosen NS-GEV model for each station over time. The shades on the graph indicate up to which degree of confidence (80%–99%) the NS-GEV model and S-GEV model return level confidence intervals are disjoint, with the color indicating whether the NS-GEV confidence interval was centered higher (red) or lower (blue) than the confidence interval of the S-GEV model.

One can note from Fig. 8 that all of the Senegal stations were significantly above the S-GEV at the beginning of the record. For the 2-year return levels (8a), only Bafing Makana in Senegal was higher than its corresponding S-GEV at the end of the data record. The uncertainty increases with longer return periods, with none of the NS-GEVs significantly higher than the S-GEV at the end of the record for 25-year return levels or greater. NS-GEV return levels for the Oualia, Kidira, Gourbassi, and Daka Saidou stations were at approximately the stationary return level at the end of the study period or below the stationary level for longer return periods. Overall, the return levels of stations in the Senegal basin spend much of the period of record significantly below the S-GEV. One can note that the difference persists into the modern period for the Bakel data series, one of the stations affected by the Manantali Dam.

For the stations in the Niger River, at the most modern data points, the 90% confidence intervals surrounding the 2 and 5-year return levels globally surpassed the confidence intervals of the stationary return values. For the Sirba and Dargol, this separation existed also at the 99% confidence level, and at the 95% confidence level for the Gorouol. The exception was the SNR series whose lower non-stationary 90% confidence bound was slightly within the upper confidence bound of the stationary value for 5-year return levels.

Fig. 9 compares the 2 and 5-year return level changes between all stations, with values normalized by each station's stationary return level (i.e. the return level estimated using the stationary GEV model, Eq. (14)). The separation in terms of return level evolution between the stations in the Senegal and Niger river basins is especially clear for the two-year return levels. The two-year return levels of the Senegal River stations (blue) start at around 1.5 times the stationary return level (y-axis = 1), reduce to as low as 0.5 during the 1980s, then increase throughout the modern period. Bakel and Kayes, the two Senegal stations affected by the Manantali Dam, have notably lower relative increases in return level values. These two stations reached to near the stationary return level value at the end of the study period, whereas the other stations all exceeded it and reaches values between 1 and 1.5 times the stationary return level. This shows the influence of the dam on trends in maximum values; one can hypothesize that without the influence of the dam, the stations Bakel and Kayes would have more closely followed the trend of the other stations that are located either upstream of the dam or on other tributaries of the Senegal River.

For the Niger River stations (red), all stations started below the stationary 2-year return level and ended well above it. For most of stations the 2-year non-stationary return levels move from less than 0.7 to more than 1.5 times the stationary return level, meaning a doubling

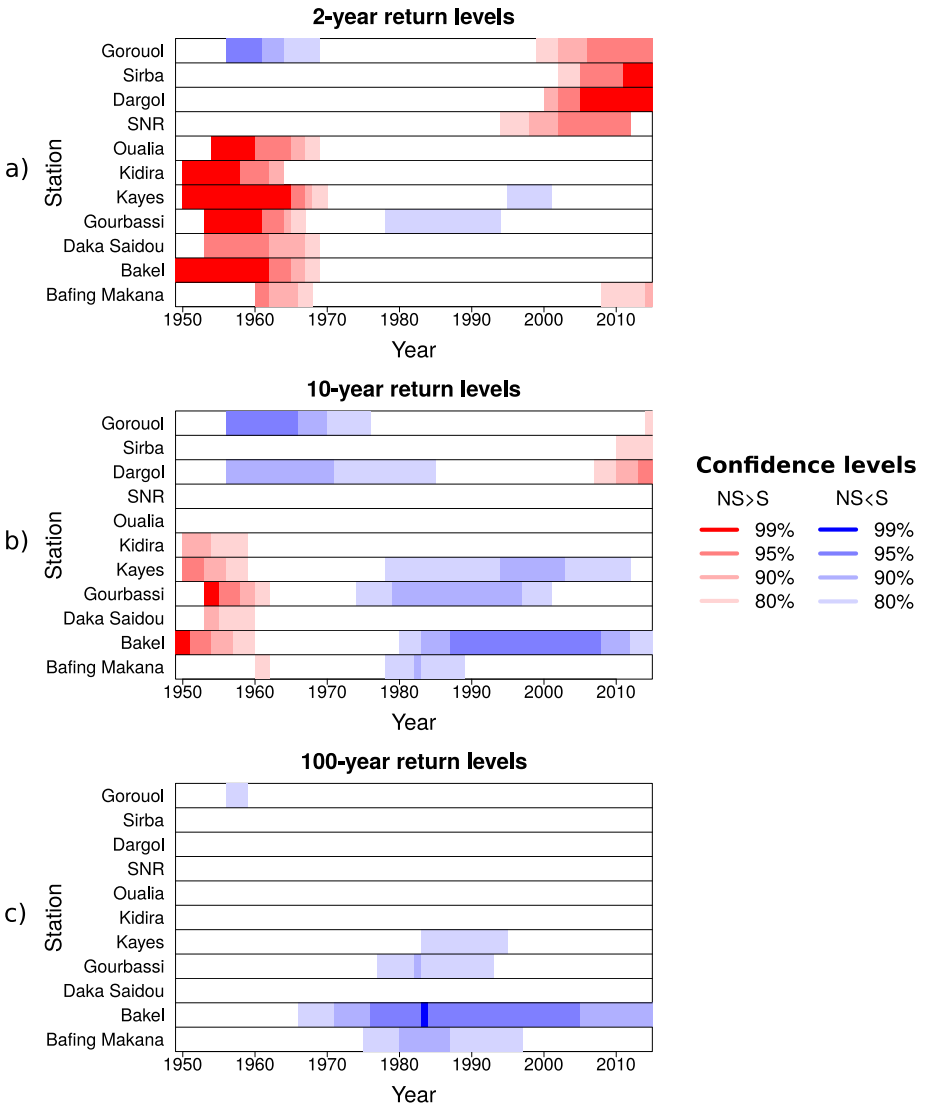

Fig. 8. Significance of the separation between NS-GEV and S-GEV models over time by station for 2-year (a), 10-year (b), and 100-year (c) return levels. The separation is measured by the overlap between the confidence intervals of the model. Red indicates that the NS-GEV was significantly higher than the S-GEV (lower bound of the NS-GEV confidence interval greater than the upper bound of the S-GEV confidence interval at a given level of confidence), whereas blue indicates that the NS-GEV was significantly lower than the S-GEV (upper bound of the NS-GEV confidence interval less than the lower bound of the S-GEV confidence interval at a given level of confidence). The shade indicates the confidence level at which the intervals are disjoint at that point in time, ranging from 80% to 99%.

discharge for a two-year return period in roughly 50 years. The SNR series in particular tripled its relative value over the study period.

As for the five-year return levels, the regional separation becomes less clear due to the greater influence of the scale parameter at higher return levels. However, the relative decreases and increases by region remained similar. Bakel and Kayes remain relatively lower than the other Senegal stations.

4.4. Scale effects of drainage area

The absolute magnitude of the increase in μ was directly correlated with the size of the drainage area of a given station. However, no correlation was found in the relation between the relative increase in μ and the drainage area. For the Sahelian Niger, a moderate correlation (Pearson's $\rho = 0.6$) was found between drainage area and return level

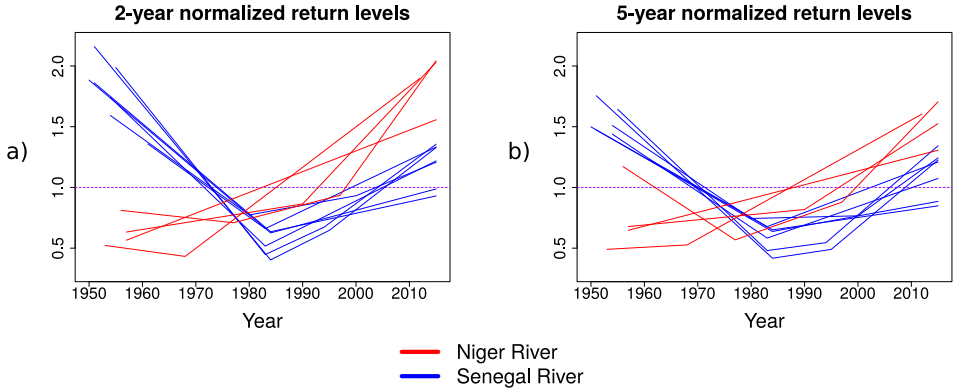

Fig. 9. Normalized two-year (a) and 5-year (b) return levels for all stations. The red lines represent Sahelian stations, and the blue lines represent Sudano-Guinean stations. (For interpretation of the references to color in this figure legend, the reader is referred to the web version of this article.)

for return periods of 25 years or longer. The trend was more evident in the Senegal basin; when the stations Bakel and Kayes were removed, the correlation was greater than 0.6 for return periods of 5 years and longer. A similar correlation ($\rho \approx 0.6$) was found between drainage area and the ξ parameter in both regions. The two-year return levels demonstrated little to no correlation with drainage area ($\rho = 0.25$). Given the limited number of data points, it is difficult to draw conclusions based on these results.

5. Discussion

5.1. Comparison of results with literature

The above results confirm the rising trend in extreme streamflow values since the 1970s and 1980s, previously found in other studies (Cassé and Gosset, 2015; Nka et al., 2015; Aich et al., 2016).

The trends found in the Guinean stations in the Senegal River basin in this study followed the trends found in Aich et al. (2016) for the Guinean stations in the Niger River basin. In both studies a decreasing trend was found until approximately the mid-1980s, followed by an increasing trend. Results are overall consistent with Nka et al. (2015)'s findings that extreme discharge is reduced in recent years compared to what it was several decades ago. The models in the present study also detected a moderate increase in recent years, whereas in Nka et al. (2015) there was no significant trend since the 1970s.

The relatively lower trends at the Kayes and Bakel stations can be explained by the construction of the Manantali Dam upstream in 1988, which would have controlled many of the larger flows. This is in agreement with the results in Faye (2015), which showed that monthly flow coefficients at Bakel were lower for peak season months in the period after dam construction than they were before dam construction. At the stations of Bafing Makana, Oualia, and Kidira, flow coefficients were higher for peak months when comparing the same time periods.

The breakpoint found at 1990 in the NS-GEV for the Dargol at Kakassi falls in between the breakpoints found by Nka et al. (2015) at 1987 (for AMAX) and 1993 (for peak over threshold values). For Sahelian stations, Aich et al. (2016) found a decreasing trend until the 1970s followed by an increasing trend. The initial decrease was found only in the SNR and Gorouol series, but all Sahelian stations tested show an increase since the 1970s. A breakpoint was found in the mid 1970s for the Sirba and early 1970s for the Gorouol, which is roughly consistent with the results in the present study.

The shifts in trends found in the SNR series (1968) and Gorouol series (1972) falls at the same point in time as the general climate shift in the late 1960s, as well as the mean discharge breakpoint identified in Tarhule et al. (2015). However, whereas the climate and mean streamflow shifts decreased after the break, the SNR series (and likewise all series for the Sahelian Niger) went from a low or negative slope to a positive slope. This is reflective of the well-documented Sahelian paradox (Albergel, 1987; Descroix et al., 2018) where locally-generated streamflow in the Sahel began increasing during the drought period, in spite of an overall reduction in rainfall.

5.2. Evaluation of the parameter ξ

In addition to the difference in timing and magnitude of trends between the Sudano-Guinean and Sahelian regions, differences in the shape parameter ξ were also found. The fact that the NS-GEVs for Sudano-Guinean stations were generally Weibull or Gumbel ($\xi \leqslant 0$) and Sahelian stations were generally Frechet ($\xi > 0$) could be due to the differences in hydrological functioning. In the Sudano-Guinean region, the flow type is Hewlettian and groundwater plays a greater role. A larger portion of the precipitation first infiltrates and contributes to river discharge at a later time, smoothing out the high spatio-temporal variability of fine-scale rainfall intensities. Flood generation is thus sensitive to both the initial conditions of the basin (groundwater storage, subsurface water, etc) and the amount of rainfall accumulated over the basin. In the Sahel, streamflow is driven by Hortonian processes (local precipitation-generated runoff) and therefore is sensitive to the intensity of rainfall at small scales. The role of initial conditions seems to be smaller in comparison to factors such as the area affected by high intensities over a short time period. These differences in the spatio-temporal scale of the processes primarily responsible for flood generation in the two regions could explain in part the differences in the tail behavior of extreme discharges between the two regions. Indeed, it is observed that rainfall at fine spatio-temporal scales (Sahelian flood generation) has heavy tail behavior (Koutsoyiannis, 2004; Panthou et al., 2012), while rainfall averaged over larger spatio-temporal scales (Sudano-Guinean flood generation) is expected to have bounded tail behavior.

This said, great care must be taken in drawing conclusions from results for ξ as the confidence intervals are large (Table 2) and include both positive (Frechet) and negative (Weibull) values for almost all stations. The confidence intervals themselves seem to indicate a difference in tail behavior between the two regions; the lower bounds of the 95% confidence intervals for ξ in the Senegal catchments are much lower than the lower bounds in the Sahelian Niger catchments (with the exception of the Gorouol), and the upper bounds are generally lower in the Senegal basin as well (though less universally). However, due to the great overlap between the confidence intervals, it is difficult to draw conclusions with a high level of certitude.

5.3. Sensitivity analyses: robustness of the results

5.3.1. Sensitivity of the model selection process to the different tests and the p-value threshold chosen for the LRT

For three out of the eleven data series, the additional application of the LRT test modified the model selection. In all three cases, the model became simpler: the scale parameter (σ) for Bakel became stationary, the location parameter of Kayes became double linear instead of triple linear, and the Gorouol model became simple linear for μ instead of double linear.

For ten out of the eleven data series, the model selection did not change with an increase in LRT test stringency, with the p-value equaling 0.05. The only change with the stricter requirement were that σ became stationary for the SNR series.

With less strict criteria ($\alpha = 0.15$), the results more closely approximated the initial AIC selection results. σ was modeled as linear non-stationary for the Bakel station, instead of the stationary model for σ selected at the $\alpha = 0.10$ significance level. The Gorouol station became double linear for μ and stationary for σ. The Kayes station NS-GEV at the p-value of 0.15 was a double linear model for μ and a simple linear model for σ. The general trends (strongly positive over the past few decades for μ and return levels) did not change with the choice of the model.

Of note at the $\alpha = 0.15$ significance level is the triple-linear model selected for μ for Kayes. The Kayes station's flow has clearly been regulated by the installation of the Manantali dam in 1988, which may have resulted in three distinct phases over the study period rather than two.

5.3.2. Sensitivity of the model parameters to optimization methodology

The choice of MLE parameter optimization method did not have a significant impact on model parameter results, nor on model selection results. Optimization methods tested were Nelder-Mead (Nelder and Mead, 1965), BFGS (Shanno, 1970), conjugate gradients (Fletcher and Reeves, 1964), L-BFGS-B (Byrd et al., 1995), and simulated annealing (Bélisle, 1992). However, the boundary limit between breakpoints and the edge of the data series did have an impact on the selection of the breakpoint. This could be of interest as the main breakpoint in the early-mid 1980s in Senegal was less than ten years before the construction of the Manantali dam. As a triple-linear model with a distance

between breakpoints of one decade was almost selected (initial AIC model selection) for the Kayes station which is downstream of the dam, the limitation could have had an impact on model selection.

5.3.3. Additional sources of uncertainty

One source of uncertainty lies in the accuracy of the rating curves for each of the stations in this study (Jalbert et al., 2011; Morlot et al., 2014). Rating curves in regions subject to sedimentation such as the Sahelian Niger River basin risk being nonstationary in time. Rating curves may also be less accurate for extreme values if measurements of flow of comparable magnitude were not used in the rating curve calibration. Although some stations (notably Kidira, Bakel, Daka Saidou, and Niamey) included such large values, this was not the case for all stations.

However, rating curve uncertainties, while possibly influencing the specific magnitudes of results, are highly unlikely to be the cause of the consistent trends detected and thus do not alter the conclusions of the present study. Trend detection was conducted using a regional approach with two large river basins within the region and several stations within each river basin. The regional approach makes the methods robust and smooths the effect of uncertainty related to rating curves.

One can also question the influence of the choice of breakpoint on the uncertainty of the results. Sensitivity testing was performed with the Bafing Makana and SNR series over a breakpoint range of five years before and after the breakpoint of the selected model. The spread of the 95% confidence interval of the selected model (one fixed breakpoint) was compared with the spread of the global confidence interval obtained from the range of breakpoints. The area within the global confidence interval but outside the selected model's confidence interval is due to breakpoint uncertainty. Based on this, the contribution of breakpoint estimation uncertainty to the overall uncertainty is on average 13% for Bafing Makana and 15% for SNR for a breakpoint range of plus and minus five years from the selected breakpoint. It was thus verified that the primary source of uncertainty comes from the GEV calibration process performed in step 2 of subsection 3.3 (uncertainty of the η_i) and not from uncertainty about the position of the breakpoint.

6. Conclusions and implications

The preceding analysis proposed a selection of NS-GEV models for hydrological annual maxima in West Africa. In all cases, the NS-GEV model was significantly more representative of the data series than the stationary GEV model. The trend is positive since the 1970s for the Sahelian stations and the mid-1980s in the Sudano-Guinean stations, with both regions demonstrating an intensification of the hydrological signal. Certain parameters and return levels, notably the μ parameter and the 2 and 5-year return levels, surpass the values expected with a stationary model with a high level of confidence at certain stations.

The results improve over other studies by providing the underlying statistical distributions for the non- stationary data series, confidence intervals on parameter values, return level estimates, and a model selection process with robust criteria. It also compares two subregions, and notably includes an extracted data series for the cumulative Sahelian red flood inputs to the Niger River. Although West Africa is used as a test region, these analyses can be applied to hydrological time series elsewhere in the world.

The methods used in this paper have some limitations. First, only parametric models that were preselected as potential best models are evaluated, thus eliminating a large range of other potential models. Second, the study only consider breakpoints that are transitions from one linear slope magnitude to another, not abrupt shifts. Furthermore, uncertainty is high (which reflects the current reality). The methods also require a certain level of expertise for use and interpretation. Additionally, the estimated uncertainties do not take into account the uncertainty in the estimation of streamflow via rating curves, which could have a significant impact on the accuracy of extreme values (Jalbert et al., 2011; Morlot et al., 2014).

However, the methods proposed in the present study are advantageous for several reasons. It is possible to use other trend and breakpoint detection methods, but many of these tests assume that the data is normally distributed (which is not the case with extremes) and thus will not be robust with data sets consisting of extreme values. Classic breakpoint detection tests (such as the Pettitt test) may work but do not provide an estimate of the magnitude of the trend. They also do not permit the estimation of return levels, which is a significant advantage of the methods based on fitting probability distributions proposed in this paper. The power of classical trend and breakpoint tests to reject the null hypothesis when applied to extreme value series is also known to be lower than when applying tests specific to GEVs. Moreover, even if some expertise is required to use them, the R packages used in this study are freely available (Heffernan et al., 2016).

The results for the return level estimates indicate that if the stationary model were to be used, it would underestimate the current return levels in the Sahelian reaches of the Niger River. For example, the non-stationary ten-year return level for the SNR series in 2012 is $600\,m^3\,s^{-1}$ larger than the value estimated from a stationary model. For all four data series in the Sahelian Niger, at the end of the data record (2012–2015), the non-stationary 2-year return level exceeds the 5-year stationary return level, indicating an increase in frequency of events of greater magnitude.

The nonstationarity of the return levels has direct implications for hydraulic works construction and river basin management. In both Sahelian and Sudanian areas, the identified increase of 2–10-year return levels is important for small structures and might have contributed to the increasing number of damaged and destroyed bridges and roads reported over the last decades (Amani and Paturel, 2017). In the Senegal basin, an accurate estimation of higher return level values (for return periods greater than 25 years) is needed not only for the management of existing dams such as the ones at Manantali, Diama and Félou, but also for the construction of additional structures such as spillways and the hydroelectric dams planned by the Organization for the Valorization of the Senegal River (in French, OMVS, see Bonneau, 2001). As the region surrounding Niamey in the Niger Basin continues to be threatened by severe flooding, accurate return level estimates are required in order to ensure that flood protection systems can protect against a given flood. In all of the above cases, if a stationary model is used, it risks overestimating or underestimating the magnitude of river discharge.

Uncertainty remains high for longer return periods. This is largely tied to the size and variability of the data set; estimating a 100-year return level based on only 60 years of data forcibly has a high level of uncertainty. As more data is collected, uncertainty will decrease and the ability to more precisely estimate return levels for longer return periods will likely improve, provided that the data is represented by a model that best suits its trends.

Uncertainty may also be reduced with a greater understanding of flood drivers. Much speculation and study has occurred in attempt to determine the causes of the changes in flood peaks in the West Africa (Seguis et al., 2004; Leblanc et al., 2008; d'Orgeval et al., 2008; Descroix et al., 2009; Descroix et al., 2012; Descroix et al., 2018; Aich et al., 2015; Cassé and Gosset, 2015; Cassé et al., 2016). In addition to climate changes, West Africa has undergone extensive land cover changes (Loireau, 1998; Anyamba and Tucker, 2005; Descroix et al., 2009) including a considerable increase in the percentage of cultivated area from the 1950s-2000s (Cappelaere et al., 2009).

Whereas much of the "Sahelian Paradox" during the drought can be attributed to land use/land cover changes, in recent years changes in river discharge seems to correlate more with changes in precipitation. Case in point, the regional trends found in this study follow those found for mean non-zero rainfall in Senegal and the central Sahel in Blanchet et al. (2018). The issue is complex; for example, in the present study the

Sirba basin streamflow did not increase as much as that of the Dargol and Gorouol, yet it both receives more rainfall (500 mm as opposed to 400 mm annually) and had increased runoff coefficients, most likely due to the impacts of agriculture (Descroix et al., 2012). Land use and climate also have impacts at different scales (Blöschl et al., 2007).

An improved understanding of the attributed causes of trends in extremes would give guidelines for the projection of pertinent results into the future. Such an approach would require coupling NS-GEV models with projected climate and land use changes. Factors to be taken take into account are both climate projections at the scale of hydrological processes and socio-economic scenarios that allow for the estimation of the anthropic pressure on the soil and the resulting changes in hydrodynamic parameters. Projection of model results into the future, however, must be done with caution due to the potential of future shifts in trends and decadal variability not accounted for in the climate and land use trends.

We recommend that those dimensioning hydraulic works seriously consider the possibility that hydrological extremes are increasing, as this is the current evidence available. This is especially pertinent for the coming decade over which evidence supports an increasing frequency of extreme rainfall and ongoing hydrological intensification (Taylor et al., 2017; Panthou et al., 2018). With this in mind, we recommend that stakeholders design structures with a shorter design life span (10–20 years) with the assumption that extremes will most probably increase. Such structures include flumes, small urban hydraulic structures, pumps, levees, and smaller dams. For longer-life structures such as large dams and spillways, they should continue to consider all factors, including the possibility that the trend may change and decrease again. Despite the potential impacts of projected land use changes and the ongoing warming of the Sahara that triggers intense rainfall events, the decadal variability of climate in the region is also likely to continue.

In spite of the uncertainties, the present study concludes within a strict level of confidence that hydrological extremes are currently increasing, and although uncertainty about the magnitude of this increase is high, it is more concrete and certain than speculation about an unknown future. The trends are consistent for all stations within each watershed despite flow uncertainties. We advise that stakeholders place importance on the possibility of greater and more frequent flood magnitudes, especially while designing smaller structures but also for larger structures. We further recommend that they take causal factors into account, although more studies are needed in order to understand the mechanisms of flood drivers.

Acknowledgements

The research leading to these results has received funding from the NERC/DFID Future Climate For Africa program under the AMMA-2050 project, grant NE/M020428/1. This work was also supported by the French national program EC2CO-LEFE “Recent evolution of hydro-climatic hazards in the Sahel: detection and attribution.” Ansoumana Bodian benefited from a grant received from the French Embassy in Senegal which financed exchanges with other researchers. We warmly acknowledge the Niger Basin Authority (ABN) and the Organisation pour la Mise en Valeur du Fleuve Sénégal (OMVS) for providing the Niger River and Senegal River discharge data.

References

Aich, V., Koné, B., Hattermann, F.F., Paton, E.N., 2016. Time series analysis of floods across the Niger River basin. Water 8, 165.
Aich, V., Liersch, S., Vetter, T., Andersson, J., Müller, E.N., Hattermann, F.F., 2015. Climate or land use? Attribution of changes in river flooding in the Sahel zone. Water 7, 2796–2820.
Akaike, H., 1974. A new look at the statistical model identification. IEEE Trans. Autom. Control 19, 716–723.
Albergel, J., 1987. Sécheresse, désertification et ressources en eau de surface: application aux petits bassins du Burkina Faso. The influence of climate change and climatic variability on the hydrologic regime and water resources 168, 355–365.
Ali, A., Lebel, T., 2009. The Sahelian standardized rainfall index revisited. Int. J. Climatol. 29, 1705–1714.
Allan, R.P., Soden, B.J., John, V.O., Ingram, W., Good, P., 2010. Current changes in tropical precipitation. Environ. Res. Lett. 5, 025205.
Amani, A., Paturel, J.-E., 2017. Le projet de révision des normes hydrologiques en Afrique de l’Ouest et Afrique Centrale. La Météorologie 6–7. https://doi.org/10.4267/2042/61964.. URLhttp://hdl.handle.net/2042/61964.
Andersen, I., Golitzen, K.G., 2005. The Niger River Basin: A Vision for Sustainable Management. World Bank Publications.
Anyamba, A., Tucker, C.J., 2005. Analysis of Sahelian vegetation dynamics using NOAA-AVHRR NDVI data from 1981–2003. J. Arid Environ. 63, 596–614.
Arnell, N.W., Gosling, S.N., 2016. The impacts of climate change on river flood risk at the global scale. Clim. Change 134, 387–401.
Asadieh, B., Krakauer, N., 2015. Global trends in extreme precipitation: climate models versus observations. Hydrol. Earth Syst. Sci. 19, 877–891.
Beguería, S., Angulo-Martínez, M., Vicente-Serrano, S.M., López-Moreno, J.I., El-Kenawy, A., 2011. Assessing trends in extreme precipitation events intensity and magnitude using non-stationary peaks-over-threshold analysis: a case study in northeast Spain from 1930 to 2006. Int. J. Climatol. 31, 2102–2114.
Bélisle, C.J., 1992. Convergence theorems for a class of simulated annealing algorithms on ℝd. J. Appl. Probab. 29, 885–895.
Blanchet, J., Aly, C., Vischel, T., Panthou, G., Sané, Y., Kane, M.D., 2018. Trend in the co-occurrence of extreme daily rainfall in West Africa since 1950. J. Geophys. Res.: Atmos.
Blanchet, J., Molinié, G., Touati, J., 2016. Spatial analysis of trend in extreme daily rainfall in southern France. Clim. Dyn. 1–14.
Blöschl, G., Ardoin-Bardin, S., Bonell, M., Dorninger, M., Goodrich, D., Gutknecht, D., Matamoros, D., Merz, B., Shand, P., Szolgay, J., 2007. At what scales do climate variability and land cover change impact on flooding and low flows? Hydrol. Process. 21, 1241–1247.
Bodian, A., Dacosta, H., Dezetter, A., 2011. Caractérisation spatio-temporelle du régime pluviométrique du haut bassin du fleuve Sénégal dans un contexte de variabilité climatique. Physio-Géo. Géographie physique et environnement 107–124.
Bodian, A., Dacosta, H., Dezetter, A., 2013. Analyse des débits de crues et d’étiages dans le bassin versant du fleuve Sénégal en amont du barrage de Manantali. Revue du LACEEDE. Climat et développement 15, 46–56.
Bodian, A., Dezetter, A., Deme, A., Diop, L., 2016. Hydrological evaluation of TRMM rainfall over the upper Senegal River basin. Hydrology 3, 15.
Bodian, A., Ndiaye, O., Dacosta, H., 2016. Evolution des caractéristiques des pluies journalières dans le bassin versant du fleuve Sénégal: Avant et après rupture. Hydrol. Sci. J. 61, 905–913.
Bonneau, M., 2001. Programme d’optimisation de la gestion des réservoirs. Besoins en eau de l’agriculture irriguée et de l’agriculture de décrue dans la vallée du fleuve Sénégal. IRD, OMVS, Dakar, Sénégal.
Boulain, N., Cappelaere, B., Séguis, L., Favreau, G., Gignoux, J., 2009. Water balance and vegetation change in the Sahel: a case study at the watershed scale with an eco-hydrological model. J. Arid Environ. 73, 1125–1135.
Bower, S.S., 2010. Natural and unnatural complexities: flood control along Manitoba’s Assiniboine River. J. Historical Geography 36, 57–67.
Boyer, J.-F., Dieulin, C., Rouche, N., Cres, A., Servat, E., Paturel, J.-E., Mahe, G., 2006. SIEREM: an environmental information system for water resources. IAHS publication 308, 19.
Brath, A., Montanari, A., Moretti, G., 2006. Assessing the effect on flood frequency of land use change via hydrological simulation (with uncertainty). J. Hydrol. 324, 141–153.
Byrd, R.H., Lu, P., Nocedal, J., Zhu, C., 1995. A limited memory algorithm for bound constrained optimization. SIAM J. Sci. Comput. 16, 1190–1208.
Camberlin, P., Beltrando, G., Fontaine, B., Richard, Y., 2002. Pluviométrie et crises climatiques en Afrique tropicale: changements durables ou fluctuations interannuelles? Historiens et Géographes 263–273.
Cappelaere, B., Descroix, L., Lebel, T., Boulain, N., Ramier, D., Laurent, J.-P., Favreau, G., Boubkraoui, S., Boucher, M., Moussa, I.B., et al., 2009. The AMMA-CATCH experiment in the cultivated Sahelian area of south-west Niger-investigating water cycle response to a fluctuating climate and changing environment. J. Hydrol. 375, 34–51.
Cappus, P., 1960. Etude des lois de l’écoulement-Application au calcul et à la prévision des débits. La houille blanche 493–520.
Cassé, C., Gosset, M., 2015. Analysis of hydrological changes and flood increase in Niamey based on the PERSIANN-CDR satellite rainfall estimate and hydrological simulations over the 1983–2013 period. Proc. Int. Assoc Hydrol. Sci. 370, 117–123.
Cassé, C., Gosset, M., Vischel, T., Quantin, G., Tanimoun, B.A., 2016. Model-based study of the role of rainfall and land use–land cover in the changes in the occurrence and intensity of Niger red floods in Niamey between 1953 and 2012. Hydrol. Earth Syst. Sci. 20, 2841–2859.
Coles, S., Bawa, J., Trenner, L., Dorazio, P., 2001. An introduction to statistical modeling of extreme values, vol. 208 Springer.
Coles, S.G., Tawn, J.A., 1996. A Bayesian analysis of extreme rainfall data. Appl. Stat. 463–478.
Condon, L., Gangopadhyay, S., Pruitt, T., 2015. Climate change and non-stationary flood risk for the upper Truckee River basin. Hydrol. Earth Syst. Sci. 19, 159.
Cunderlik, J.M., Burn, D.H., 2003. Non-stationary pooled flood frequency analysis. J. Hydrol. 276, 210–223.
Dai, A., Trenberth, K.E., Qian, T., 2004. A global dataset of Palmer Drought Severity Index for 1870–2002: relationship with soil moisture and effects of surface warming. J. Hydrometeorol. 5, 1117–1130.
Davison, A.C., Hinkley, D.V., 1997. Bootstrap methods and their application, vol. 1 Cambridge University Press.
Descroix, L., Genthon, P., Amogu, O., Rajot, J.-L., Sighomnou, D., Vauclin, M., 2012.

Change in Sahelian rivers hydrograph: The case of recent red floods of the Niger River in the Niamey region. Global Planet. Change 98, 18–30.
Descroix, L., Guichard, F., Grippa, M., Lambert, L.A., Panthou, G., Mahé, G., Gal, L., Dardel, C., Quantin, G., Kergoat, L., Bouaïta, Y., Hiernaux, P., Vischel, T., Pellarin, T., Faty, B., Wilcox, C., Malam Abdou, M., Mamadou, I., Vandervaere, J.-P., Diongue-Niang, A., Ndiaye, O., Sané, Y., Dacosta, H., Gosset, M., Cassé, C., Sultan, B., Barry, A., Amogu, O., Nka Nnomo, B., Barry, A., Paturel, J.-E., 2018. Evolution of surface hydrology in the sahelo-sudanian strip: an updated review. Water 10.
Descroix, L., Mahé, G., Lebel, T., Favreau, G., Galle, S., Gautier, E., Olivry, J., Albergel, J., Amogu, O., Cappelaere, B., et al., 2009. Spatio-temporal variability of hydrological regimes around the boundaries between Sahelian and Sudanian areas of West Africa: a synthesis. J. Hydrol. 375, 90–102.
Di Baldassarre, G., Montanari, A., Lins, H., Koutsoyiannis, D., Brandimarte, L., Blöschl, G., 2010. Flood fatalities in Africa: from diagnosis to mitigation. Geophys. Res. Lett. 37.
Diop, L., Yaseen, Z.M., Bodian, A., Djaman, K., Brown, L., 2017. Trend analysis of streamflow with different time scales: a case study of the upper Senegal River. ISH J. Hydraul. Eng. 1–10.
d'Orgeval, T., Polcher, J., Rosnay, P.d., 2008. Sensitivity of the West African hydrological cycle in ORCHIDEE to infiltration processes. Hydrol. Earth Syst. Sci. 12, 1387–1401.
Efron, B., 1979. Computers and the theory of statistics: thinking the unthinkable. SIAM Rev. 21, 460–480.
Efron, B., Tibshirani, R.J., 1994. An Introduction to the Bootstrap. CRC Press.
Elmer, F., Hoymann, J., Düthmann, D., Vorogushyn, S., Kreibich, H., 2012. Drivers of flood risk change in residential areas. Nat. Hazards Earth Syst. Sci. 12, 1641–1657.
Erb, K.-H., Lauk, C., Kastner, T., Mayer, A., Theurl, M.C., Haberl, H., 2016. Exploring the biophysical option space for feeding the world without deforestation. Nat. Commun. 7, 11382.
Favreau, G., Cappelaere, B., Massuel, S., Leblanc, M., Boucher, M., Boulain, N., Leduc, C., 2009. Land clearing, climate variability, and water resources increase in semiarid southwest Niger: a review. Water Resour. Res. 45.
Faye, C., 2015. Impact du changement climatique et du barrage de Manantali sur la dynamique du régime hydrologique du fleuve Sénégal à Bakel (1950–2014). BSGLg.
Fletcher, R., Reeves, C.M., 1964. Function minimization by conjugate gradients. Comput. J. 7, 149–154.
Gal, L., Grippa, M., Hiernaux, P., Pons, L., Kergoat, L., 2017. The paradoxical evolution of runoff in the pastoral Sahel: analysis of the hydrological changes over the Agoufou watershed (Mali) using the KINEROS-2 model. Hydrol. Earth Syst. Sci. 21, 4591.
Gascon, T., Vischel, T., Lebel, T., Quantin, G., Pellarin, T., Quatela, V., Leroux, D., Galle, S., 2015. Influence of rainfall space-time variability over the Ouémé basin in Benin. Proc. Int. Assoc. Hydrol. Sci. 368, 102–107.
Guillot, P., 1993. The arguments of the gradex method: a logical support to assess extreme floods. IAHS Publication pp. 287–287.
Gumbel, E., 1957. Extreme values in technical problems. Technical Report Technical report T-7A, Department of Engineering, Columbia Univ., Press, New York, AD120920.
Heffernan, J.E., Stephenson, A.G., Gilleland, E., 2016. ismev: An Introduction to Statistical Modeling of Extreme Values. URLhttps://CRAN.R-project.org/package=ismev r package version 1.41.
Hewlett, J.D., 1961. Soil moisture as a source of base flow from steep mountain watersheds, Forest Service, Southeastern Forest Experiment Station. US Department of Agriculture.
Hewlett, J.D., Hibbert, A.R., 1967. Factors affecting the response of small watersheds to precipitation in humid areas. Forest Hydrol. 1, 275–290.
Hirabayashi, Y., Mahendran, R., Koirala, S., Konoshima, L., Yamazaki, D., Watanabe, S., Kim, H., Kanae, S., 2013. Global flood risk under climate change. Nat. Clim. Change 3, 816.
Horton, R.E., 1933. The role of infiltration in the hydrologic cycle. Eos, Trans. Am. Geophys. Union 14, 446–460.
Hosking, J.R.M., Wallis, J.R., 1997. Regional Frequency Analysis: An Approach Based on L-moments. Cambridge University Press.
Jalbert, J., Mathevet, T., Favre, A.-C., 2011. Temporal uncertainty estimation of discharges from rating curves using a variographic analysis. J. Hydrol. 397, 83–92.
Kahle, D., Wickham, H., 2013. ggmap: spatial visualization with ggplot2. R J. 5, 144–161. URLhttp://journal.r-project.org/archive/2013-1/kahle-wickham.pdf.
Katz, R.W., Parlange, M.B., Naveau, P., 2002. Statistics of extremes in hydrology. Adv. Water Resour. 25, 1287–1304.
Kim, H., Kim, S., Shin, H., Heo, J.-H., 2017. Appropriate model selection methods for nonstationary generalized extreme value models. J. Hydrol. 547, 557–574.
Koutsoyiannis, D., 2004. Statistics of extremes and estimation of extreme rainfall: II. Empirical investigation of long rainfall records/Statistiques de valeurs extrêmes et estimation de précipitations extrêmes: II. Recherche empirique sur de longues séries de précipitations. Hydrol. Sci. J. 49.
Kundzewicz, Z., Graczyk, D., Maurer, T., Pińskwar, I., Radziejewski, M., Svensson, C., Szwed, M., 2005. Trend detection in river flow series: 1. Annual maximum flow/Détection de tendance dans des séries de débit fluvial: 1. Débit maximum annuel. Hydrol. Sci. J. 50.
Kundzewicz, Z.W., Ulbrich, U., Graczyk, D., Krüger, A., Leckebusch, G.C., Menzel, L., Pińskwar, I., Radziejewski, M., Szwed, M., et al., 2005. Summer floods in central Europe–climate change track? Nat. Hazards 36, 165–189.
Lamb, P.J., 1983. Sub-saharan rainfall update for 1982; continued drought. Int. J. Climatol. 3, 419–422.
Lambin, E.F., Geist, H.J., Lepers, E., 2003. Dynamics of land-use and land-cover change in tropical regions. Ann. Rev. Environ. Resour. 28, 205–241.
Le Barbé, L., Lebel, T., 1997. Rainfall climatology of the HAPEX-Sahel region during the years 1950–1990. J. Hydrol. 188, 43–73.
Le Barbé, L., Lebel, T., Tapsoba, D., 2002. Rainfall variability in West Africa during the years 1950–90. J. Clim. 15, 187–202.
Lebel, T., Ali, A., 2009. Recent trends in the Central and Western Sahel rainfall regime (1990–2007). J. Hydrol. 375, 52–64.
Lebel, T., Diedhiou, A., Laurent, H., 2003. Seasonal cycle and interannual variability of the Sahelian rainfall at hydrological scales. J. Geophys. Res.: Atmos. 108.
Leblanc, M.J., Favreau, G., Massuel, S., Tweed, S.O., Loireau, M., Cappelaere, B., 2008. Land clearance and hydrological change in the Sahel: Southwest Niger. Global Planet. Change 61, 135–150.
L'hote, Y., Mahé, G., Somé, B., Triboulet, J.P., 2002. Analysis of a Sahelian annual rainfall index from 1896 to 2000; the drought continues. Hydrol. Sci. J. 47, 563–572.
Li, K., Coe, M., Ramankutty, N., De Jong, R., 2007. Modeling the hydrological impact of land-use change in West Africa. J. Hydrol. 337, 258–268.
Loireau, M., 1998. Espaces-Ressources-Usages: Spatialisation des interactions dynamiques entre les systèmes sociaux et les systèmes écologiques au Sahel nigérien (Ph.D. thesis). Université de Montpellier 3.
Ly, M., Traore, S.B., Alhassane, A., Sarr, B., 2013. Evolution of some observed climate extremes in the West African Sahel. Weather Clim. Extremes 1, 19–25.
Mahé, G., Olivry, J.-C., Dessouassi, R., Orange, D., Bamba, F., Servat, E., 2000. Relations eaux de surface–eaux souterraines d'une rivière tropicale au Mali. Comptes Rendus de l'Académie des Sciences-Series IIA-Earth and Planetary Science 330, 689–692.
Mahé, G., Olivry, J.C., & Servat, E. (2005). Sensibilité des cours d'eau ouest-africains aux changements climatiques et environnementaux: extrêmes et paradoxes. In: Frank, S., Wagener, T., Bgh, E., Gupta, H.V., Bastidas, L., Nobre, C., de Oliveira Galvão, C., (Eds.), Regional Hydrological Impacts of Climatic Change-Hydroclimatic Variability, pp. 169–177.
Mahé, G., Paturel, J.-E., 2009. 1896–2006 Sahelian annual rainfall variability and runoff increase of Sahelian rivers. C.R. Geosci. 341, 538–546.
Mamadou, I., Gautier, E., Descroix, L., Noma, I., Moussa, I.B., Maiga, O.F., Genthon, P., Amogu, O., Abdou, M.M., Vandervaere, J.-P., 2015. Exorheism growth as an explanation of increasing flooding in the Sahel. Catena 131, 130–139.
Marty, C., Blanchet, J., 2012. Long-term changes in annual maximum snow depth and snowfall in Switzerland based on extreme value statistics. Clim. Change 111, 705–721.
Milly, P.C., Betancourt, J., Falkenmark, M., Hirsch, R.M., Kundzewicz, Z.W., Lettenmaier, D.P., Stouffer, R.J., 2008. Stationarity is dead: whither water management? Science 319, 573–574.
Morlot, T., Perret, C., Favre, A.-C., Jalbert, J., 2014. Dynamic rating curve assessment for hydrometric stations and computation of the associated uncertainties: quality and station management indicators. J. Hydrol. 517, 173–186.
Nelder, J.A., Mead, R., 1965. A simplex method for function minimization. Comput. J. 7, 308–313.
Nicholson, S., 2013. The West African Sahel: a review of recent studies on the rainfall regime and its interannual variability. ISRN Meteorol. 2013, 1–32.
Nicholson, S.E., 2000. The nature of rainfall variability over Africa on time scales of decades to millenia. Global Planet. Change 26, 137–158.
Nka, B., Oudin, L., Karambiri, H., Paturel, J.-E., Ribstein, P., 2015. Trends in floods in West Africa: analysis based on 11 catchments in the region. Hydrol. Earth Syst. Sci. 19, 4707–4719.
O'Gorman, P.A., 2012. Sensitivity of tropical precipitation extremes to climate change. Nat. Geosci. 5, 697–700.
Olsen, J.R., Lambert, J.H., Haimes, Y.Y., 1998. Risk of extreme events under nonstationary conditions. Risk Anal. 18, 497–510.
Ozer, P., Hountondji, Y., Laminou Manzo, O., 2009. Evolution des caractéristiques pluviométriques dans l'est du Niger de 1940 à 2007. Geo-Eco-Trop 33, 11–30.
Panthou, G., Lebel, T., Vischel, T., Quantin, G., Sane, Y., Ba, A., Ndiaye, O., Diongue-Niang, A., Diopkane, M., 2018. Rainfall intensification in tropical semi-arid regions: the sahelian case. Environ. Res. Lett. 13, 064013.
Panthou, G., Vischel, T., Lebel, T., 2014. Recent trends in the regime of extreme rainfall in the Central Sahel. Int. J. Climatol. 34, 3998–4006.
Panthou, G., Vischel, T., Lebel, T., Blanchet, J., Quantin, G., Ali, A., 2012. Extreme rainfall in West Africa: a regional modeling. Water Resour. Res. 48.
Panthou, G., Vischel, T., Lebel, T., Quantin, G., Pugin, A.-C.F., Blanchet, J., Ali, A., 2013. From pointwise testing to a regional vision: an integrated statistical approach to detect nonstationarity in extreme daily rainfall. application to the Sahelian region. J. Geophys. Res.: Atmos. 118, 8222–8237.
Paquet, E., Garavaglia, F., Garçon, R., Gailhard, J., 2013. The SCHADEX method: a semi-continuous rainfall–runoff simulation for extreme flood estimation. J. Hydrol. 495, 23–37.
Park, J.-S., Kang, H.-S., Lee, Y.S., Kim, M.-K., 2011. Changes in the extreme daily rainfall in South Korea. Int. J. Climatol. 31, 2290–2299.
Population-Reference-Bureau, 2016. 2016 world population data sheet with a special focus on human needs and sustainable resources.
Re, M., Barros, V.R., 2009. Extreme rainfalls in SE South America. Clim. Change 96, 119–136.
Rochette, C. et al., 1974. Le bassin du fleuve Senegal. ORSTOM.
Samimi, C., Fink, A., Paeth, H., 2012. The 2007 flood in the Sahel: causes, characteristics and its presentation in the media and FEWS NET. Nat. Hazards Earth Syst. Sci. 12, 313.
Sanogo, S., Fink, A.H., Omotosho, J.A., Ba, A., Redl, R., Ermert, V., 2015. Spatio-temporal characteristics of the recent rainfall recovery in West Africa. Int. J. Climatol. 35, 4589–4605.
Seguis, L., Cappelaere, B., Milési, G., Peugeot, C., Massuel, S., Favreau, G., 2004. Simulated impacts of climate change and land-clearing on runoff from a small Sahelian catchment. Hydrol. Process. 18, 3401–3413.
Shanno, D.F., 1970. Conditioning of quasi-Newton methods for function minimization. Math. Comput. 24, 647–656.

Sighomnou, D., Descroix, L., Genthon, P., Mahé, G., Moussa, I.B., Gautier, E., Mamadou, I., Vandervaere, J.-P., Bachir, T., Coulibaly, B., et al., 2013. La crue de 2012 à Niamey: un paroxysme du paradoxe du Sahel? Science et changements planétaires/Sécheresse 24, 3–13.

Tarhule, A., 2005. Damaging rainfall and flooding: the other Sahel hazards. Clim. Change 72, 355–377.

Tarhule, A., Zume, J.T., Grijsen, J., Talbi-Jordan, A., Guero, A., Dessouassi, R.Y., Doffou, H., Kone, S., Coulibaly, B., Harshadeep, N.R., 2015. Exploring temporal hydroclimatic variability in the Niger Basin (1901–2006) using observed and gridded data. Int. J. Climatol. 35, 520–539.

Taylor, C.M., Belušić, D., Guichard, F., Parker, D.J., Vischel, T., Bock, O., Harris, P.P., Janicot, S., Klein, C., Panthou, G., 2017. Frequency of extreme Sahelian storms tripled since 1982 in satellite observations. Nature 544, 475.

Tschakert, P., Sagoe, R., Ofori-Darko, G., Codjoe, S.N., 2010. Floods in the Sahel: an analysis of anomalies, memory, and anticipatory learning. Clim. Change 103, 471–502.

Villarini, G., Serinaldi, F., Smith, J.A., Krajewski, W.F., 2009. On the stationarity of annual flood peaks in the continental United States during the 20th century. Water Resour. Res. 45.

Vischel, T., Lebel, T., 2007. Assessing the water balance in the Sahel: Impact of small scale rainfall variability on runoff. Part 2: Idealized modeling of runoff sensitivity. J. Hydrol. 333, 340–355.